Additive Manufacturing of Titanium Alloys for Biomedical Applications

Lai-Chang Zhang and Yujing Liu

1 Introduction

More than 90% of patients over the age of 40 suffer from varying degrees of joint disease. For patients with advanced arthritis, artificial implants made from biomedical materials help release pain and increase people's life [1]. All of these require orthopaedic surgery, resulting in an increasing number of replacements. Biomedical applications are designed and fabricated primarily in accordance with the requirements of the implant and are commonly used in different parts of the body. The ultimate goal of the researchers is to complete the implantation of the human body without failure or modification of the operation. Therefore, the choice of materials is significant and need to be given priority consideration. Such a material should have the following advantages in human body fluid environment including great corrosion resistance, high strength, low Young's modulus, good wear resistance and no cytotoxicity. So far, three common metals have been used for implants, i.e. stainless steel, Co based alloys and titanium alloys [2, 3]. Titanium alloys have been extensively studied on the basis of excellent mechanical properties such as the light weight, high strength, corrosion resistance, good biocompatibility and low modulus [4–7]. Conventional titanium alloy manufacturing methods such as casting and powder metallurgy need subsequent mechanical processing, which consumes more time and energy.

Titanium alloys are usually manufactured through casting technology, powder metallurgy technology and foaming technology [8, 9]. However, these traditional techniques involve multiple processing steps, requiring longer periods of time, as well as more material resource and energy consumption [10]. In addition, the high reactivity of titanium and oxygen and its high melting point bring some challenges to

L.-C. Zhang (✉) · Y. Liu
Edith Cowan University, Perth, WA, Australia
e-mail: l.zhang@ecu.edu.au

B. AlMangour (ed.), *Additive Manufacturing of Emerging Materials*,
https://doi.org/10.1007/978-3-319-91713-9_5

these typical technologies. Compared with many other metal alloys, the complexity of the extraction process, the difficulty of melting, the manufacturing and mechanical problems make the titanium alloys expensive. The material removal from the traditional multistep manufacturing process is difficult. High cost and difficult processing are the two main reasons that titanium alloy is difficult to be widely used. The porous structure method is very necessary for the manufacture of the parts with complex shapes.

In recent decades, the development of additive manufacturing (AM) technology has stimulated and improved the development of the implants [11–14]. The porous implants can be produced directly from the additive manufacturing system without any subsequent processing program. These implants have obvious advantages, such as low Young's modulus and light weight, which can promote the ingrowth of bone cells. Compared with the conventional methods, additive manufacturing can realize the pore structure of complex unit structure by precision machining, which has aroused great concerns. Until now, selective laser melting (SLM) and electron beam melting (EBM) are the two most common additive manufacturing technologies used for manufacturing metal components [7]. The parts produced could have complex structures and have high mechanical properties. The combination of additive manufacturing technology and high performance biomedical titanium materials will help to succeed in the field of implants. This paper mainly focuses on the development of biomedical titanium alloys and their AM as-produced parts as a medical implant.

2 Additive Manufacturing for Biomedical Application

Additive Manufacturing, commonly referred to as 3D printing, is a method of fabricating objects from three-dimensional model data based on the principle, by melting a layer of powder using a laser or electron beam, Through the computer control to produce the structure of complex components [7]. Due to its rapid, efficient and accurate control of the internal pore structure and the complex shape of the produced components, additive manufacturing has been widely concerned in the fields of aerospace and biomedicine. Generally, there are two representative additive manufacturing techniques, i.e. selective laser melting and electron beam melting [7]. In this part, the additive manufacturing working principle and production process (including selective laser melting and electron beam melting), microstructure, mechanical properties of as-produced products and their applications in biomedical field are briefly discussed.

2.1 Selective Laser Melting (SLM)

Selective laser melting system was first reported by Fraunhofer Institute ILT in Aachen in 1995 in Germany. Differently, selective laser melting systems use a laser spot as an input energy to completely melt the powder bed, which was deposited on the metal plate in advance. The computer controls the laser beam through two mirrors and then the laser beam is focused on the powder bed. The input laser beam with a high energy of up to 1 kW and the mechanical movements of the scanning mirror permit accurate laser beam scanning up to ~15 m/s scan rate to make sure the powder melted completely [15]. The processing chamber is filled with argon gas atmosphere during manufacturing process to avoid occurrence of oxidation [16]. So far, a wide range of materials including metals, polymers and ceramic [8, 17–21] have been used for industry applications. The SLM-produced components including the solid parts and complex porous structures exhibit excellent mechanical properties without subsequent treatment [22, 23].

The main goal of the selective laser melting is to obtain completely dense and defect-free parts. However, achieving this goal is not easy because of the absence of mechanical stress in the selective laser melting, which is dominated by gravity, recoil forces, melt pool surface tension and thermal effects [7]. The selective laser melting process involves a large number of process parameters, so proper control of the relevant parameters will result in a high quality product. Some parameters, such as laser wavelength and laser operating mode, cannot be changed for a specific selective laser melting system. In addition, certain properties of the powder, such as surface tension and thermal conductivity, which defines the boundary conditions for the selective laser melting process, are fixed. In contrast, other parameters, called manufacturing or process parameters, can be calculated and optimized [11]. Many previous articles have studied and optimized in details for processing parameters of some specific materials.

In general, for a given material, the laser energy density, E, applied to a certain volume of powder material during selective laser melting is defined by

$$\mathrm{E} = \frac{P}{vts} \tag{1}$$

where P is the input power, v is the scanning speed, t is the layer thickness and s is the hatch space. A near-full density component can be obtained by a group of optimized parameters which balance all factors above during selective laser melting process. As can be seen in Eq. 1, increasing the input power and/or reducing the scan speed or layer thickness or scan hatch space can rise the laser energy density, thereby increasing the temperature of the melt pool. A higher laser energy density will result in a larger amount of melting area and therefore higher final density [10]. Since the formation of a complete melting is a necessary condition for the manufacture of dense parts, obtaining high-density parts requires sufficient laser energy density. Laser energy density is a key factor that affects the densification and quality of SLM-made parts. For a given material, the value of the energy density can be

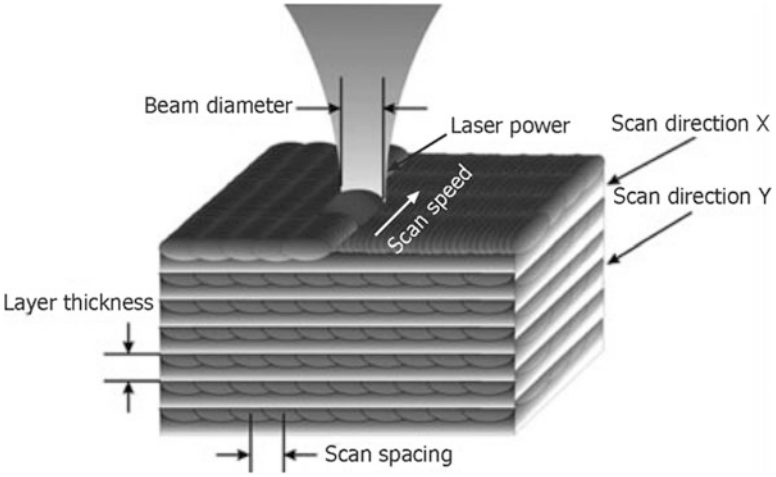

Fig. 1 Schematic of selective laser melting parameters [24]

precisely calculated from the known processing parameters. The optimized energy density usually has a range rather than a fixed value. In general, the minimum critical laser energy density produces the densest part. For example, the critical laser energy densities (CP-Ti, Ti-6Al-4V and Ti2448 of pure titanium with selective laser melting are around 120 and 40 J/mm^3, respectively [25]. A schematic of these selective laser melting processing parameters is shown in Fig. 1. In selective laser melting, the laser beam travels to the powder bed at a constant rate, called scanning speed (v), which controls the selective laser melting production time. In other words, if you need a short production time, you need a higher scanning speed. However, the maximum laser power for a particular selective laser melting device must be taken into account when increasing the scan speed [25]. Layer thickness defines the energy required to melt/solidify a layer of powder and the production time. The thickness of the layer is very important, as good inter-layer connectivity is only possible when previously processed layers are re-melted. If a larger layer thickness is used in the SLM process, the production time of manufacturing a component can be reduced. However, higher energy inputs also require full melting of the thick layer, which can result in increasing surface roughness and reducing dimensional accuracy. The scanning distance (s) is usually chosen parallel to the selective laser melting line, so it is also named as "hatch space" [25]. Scanning strategy is laser scanning track referred to the scanning length and pattern, the pattern can be a straight line or a circle. There are several common scanning strategies including cross-hatching zigzag scanning pattern, unidirectional scanning, inter-layer scanning and interlayer rotation scanning (Fig. 2). For a give material, different strategies will result in different relative density and mechanical properties; for example, the relative density of SLM-produced Ti-6Al-4V samples with cross-hatching zigzag scanning pattern can reach 99.9% [25].

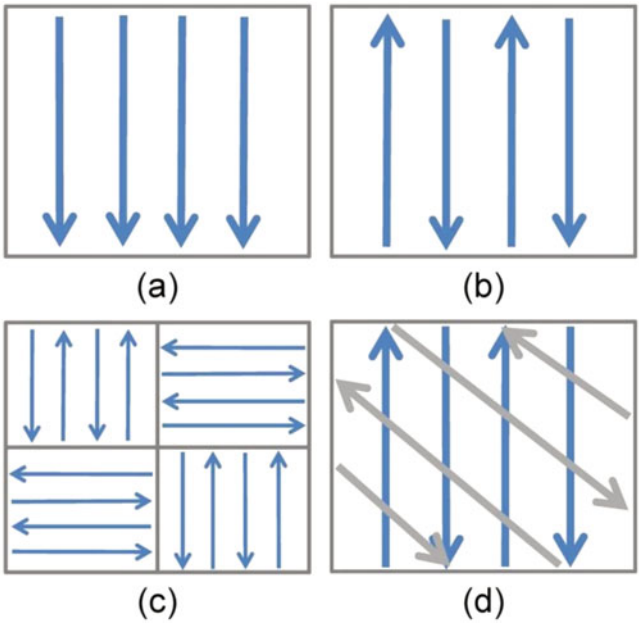

Fig. 2 Different selective laser melting processing patterns: (**a**) Uni-directional scanning, (**b**) Bi-directional scanning, (**c**) Inter-layer scanning, and (**d**) Interlayer rotation scanning [26]

2.2 Electron Beam Melting (EBM)

Electron beam melting is another AM system equipped with an electron beam launching device, which can produce nearly full density parts in a vacuum environment [29, 30]. The working principle and process of electron beam melting are similar to that of selective laser melting (Fig. 3) [27, 28]. The main difference with the selective laser melting is that the electron beam melting uses different heat source and chamber atmosphere. The heat source of electron beam melting is electron beam with a voltage of 60 kV, which preheats the substrate plate to a pre-setting temperature before dropping the powder [6, 7]. The electron beam will prescan the powder for sintering the powder and then scan the powder bed based on the sample CAD geometric shape. These differences in beam energy input and chamber environment of electron beam melting and selective laser melting result in the different microstructure (referred to melt pool size, phase type and grain size) and mechanical properties (referred to hardness, compressive, tensile and fatigue properties) of selective laser melting and electron beam melting products. The densification rate and microstructural homogeneity of EBM-produced part with an optimized parameter results in an improvement of relative density and mechanical properties [6, 7]. Some studies have been conducted to study the performance of EBM as-fabricated components and improve the properties of those samples. Some previous works have reported that plenty of implants such as knee, hip joint, and jaw replacements have been produced successfully by electron beam melting.

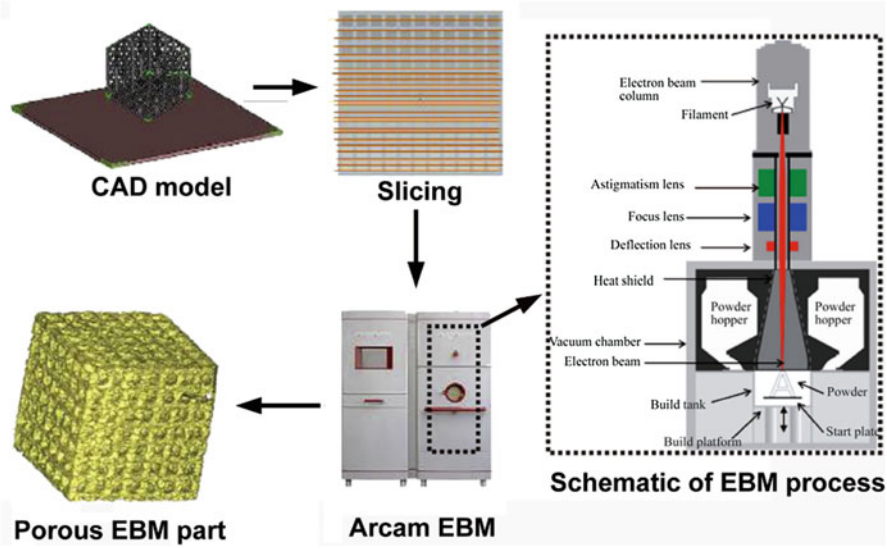

Fig. 3 Schematic diagram of electron beam melting system [27, 28]

3 Development of AM Biomedical Titanium Alloy

The ideal goal of researchers is to get a material that can be implanted into the human body for a long time without reoperation. Therefore, the performance of materials is considered a priority. Such a material should have the advantages of strong corrosion resistance, high strength, low modulus of elasticity, good wear resistance and no cytotoxicity in human environment [25, 29]. Among the three common metal materials used in medical field, titanium alloys have excellent mechanical properties in terms of low density, high strength, excellent corrosion resistance, good biocompatibility and low modulus [25, 29]. As a result, they prefer biomedical applications because they have good performance.

It is reported that the first titanium and its alloys were developed in the United States in 1940s [25]. Until now, titanium alloys have been widely used in aerospace, chemical and medical industries. Different titanium alloys also have different properties. For example, commercially pure titanium has good biocompatibility, but its low strength (~500MPa) limits its wide application [9]. In the past few decades, a lot of efforts have been made to develop titanium based alloys with excellent mechanical properties and excellent biocompatibility. At present, the most commonly used titanium alloy is an $\alpha + \beta$ type Ti-6Al-4V, originally developed for aerospace industry. Subsequent research had found that it has excellent corrosion resistance and high strength making it an ideal choice for biomaterials. Zhang et al. [31] reported that the cell had a very high survival rate on the thin disk fabricated by Ti-6Al-4V alloy. Johansson et al. [32] showed that Ti-6Al-4V also applied to the soft tissue of rats after implantation. However, recent studies [16, 33] shows the adverse

properties, including some cytotoxic components such as Al and V, which are associated with neurotoxicity and neurodegenerative diseases [34]. Furthermore, Ti-6Al-4V presents much higher elastic modulus (~110 GPa) compared to human bone (less than 30 GPa), this can cause stress shielding, resulting in bone loss and premature failure. Some researchers reported that β-type titanium alloys composing of non-toxic elements with low modulus are good materials for potential applications as implant [35].

The β phase of titanium alloys, which is metastable under the β/α transition temperature, can be reserved at room temperature through introducing some β stabilizer elements, for example, the elements of Nb, Ta, Mo, Zr and Sn can be used for producing βtitanium alloys. Due to their non-toxic property, these alloys can be manufactured as implants to pursue an improvement of long-term performance [1, 36]. Synthes et al. [37] made a comparison for the performance of Ti-7.5Mo, Ti-15Mo, Ti-10Mo and Ti-13Nb-13Zr, and considered Ti-15Mo alloy as potential of medical material with fine microstructure, high strength and low modulus. After systematical study, Ho et al. [38] pointed out that the Ti-15Mo comprised the low modulus with a value of ~77 GPa. Furthermore, some β type TiNb-based alloys presented the super elasticity; for example, Kim et al. [39] observed the super elasticity in Ti-(15–35) (at.%) Nb alloys with a recoverable strain of 3.3%, this excellent performance expands the scope of application of TiNb-based alloys. Hao et al. found that Ti-24Nb-4Zr-7.5Sn alloy had the lowest Young's modulus of 52 GPa and great super elasticity at room temperature [40]. The following studies reported that Ti2448 alloy in the as hot-rolled state exhibited peculiar non-linear super-elastic behaviour with the greatest recoverable strain up to 3.3% and incipient Young's modulus of 42 GPa. Until now, many titanium alloys have been processed by AM technologies. The materials, manufacturing methods and their mechanical properties are listed in Table 1.

3.1 Selective Laser Melting (SLM) of Titanium Alloys

Selective laser melting is able to successfully produce a variety of titanium alloys, such as commercially pure titanium (CP-Ti), Ti-6Al-4V and Ti-24Nb-4Zr-8Sn (Ti2448), and some of the them have been well applied in medical field [50]. As a traditional implant material, CP-Ti is one of the most commonly used titanium alloys in AM printing medical applications. SLM as-produced CP–Ti samples mostly demonstrate the importance of manufacturing parameters, microstructures and mechanical properties [11]. It was reported that the input energy density (E) of 120 J/mm^3 is suitable to melt the powders sufficiently and build almost fully dense CP-Ti parts with the relative density is high than 99.5% [51]. However, the input power and scan speed should be adjusted at this energy density for achieving high-density parts (Fig. 4).

Laser processing parameters affect the microstructures of the SLM-produced CP-Ti samples, variation from plate-like α to acicular martensitic α' phase (Fig. 5)

Table 1 The mechanical properties of EBM-manufactured titanium materials

Material	Method	UTS (MPa)	$\sigma_{0.2}$ (MPa)	Elongation (%)	Hardness (GPa)	E (GPa)	References
Cp-Ti	SLM	757	555	19.5	2.61	106 ± 3	[9]
Cp-Ti	SLM	650	500	17			[41]
Ti–6Al–4V	SLM	1267	1110	7.28	4.09	109	[42]
Ti-24Nb-4Zr-7.9Sn (Ti2448)	SLM	665 ± 18	563 ± 38	13.8 ± 4.1	2.2	53	[16]
Ti–6Al–4V	EBM	950–990	910–940	14–16	…	120	[27]
Ti–6Al–4V	EBM	910 ± 10	830 ± 5	…	3.21 ± 0.02	118 ± 5	[43]
Ti–6Al–4V	EBM	1100–1400	…	12–25	4.3	…	[44]
Ti–6Al–4V	EBM	1150–1200	1100–1150	16–25	3.6–3.9	…	[45]
Ti–6Al–4V	EBM	775	735	2.3	3.69	93	[46]
Ti–6Al–4V	EBM	994–1029	883–938	11.6–13.6	…	…	[41]
Ti–6Al–4V	EBM	930	865	12–17	…	…	[47]
Ti–6Al–4V	EBM	944.5–964.5	823.4–851.8	13.2–16.3	3.19–3.27	…	[12]
Ti–6Al–4V	EBM	…	832–1049	…	…	…	[5]
Ti–6Al–4V	EBM	~990–1180	~900–1100	~18–23	…	…	[13]
Ti-48Al-2Nb-0.7Cr-0.3Si	EBM	336 ± 26	253 ± 13	0.27 ± 0.1	…	166 ± 2	[48]
γ-TiAl	EBM	…	1400	…	4.1	…	[29]
Ti-24Nb-4Zr-7.9Sn (Ti2448)	EBM	…	…	…	2.5	…	[49]

UTS is the ultimate tensile strength; $\sigma_{0.2}$ is yield strength; and E is Young's modulus

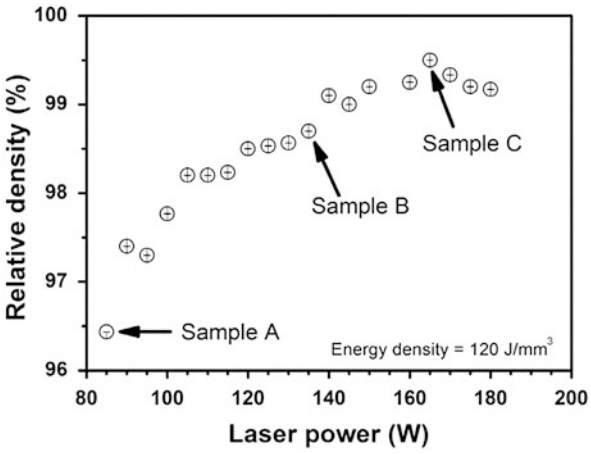

Fig. 4 Relationship between relative density and laser power for the SLM-fabricated CP–Ti parts at fixed energy density of 120 J/mm^3. Samples A, B, and C show different examples of relative densities [9]

which can be determined by different laser scan speed (v). With a constant input energy density (E) of 120 J/mm^3, once the laser scan speed is lower than 100 mm/s complete allotropic transformation of β to a takes place in the process of solidification because of energy thermalization in the melt pool (Fig. 5a). On the other hand, with increasing the laser scan speed over 100 mm/s, both kinetic and thermal characteristics below cooling go up, resulting in the growth in temperature gradients in the melt pool [60], and thereby causing the generation of α' in the final SLM-produced sample (Fig. 5).

As mentioned earlier, Ti–6Al–4V is another commonly used titanium alloy with an (α + β)-type phase in medical field. Literature showed that SLM as-produced Ti–6Al–4V samples are composed of dominant fine acicular α' martensite and some prior β grains [26, 52]. This microstructure is different with the typical α + β morphology of Grade 5 sample (Fig. 6). SLM-produced sample comprising acicular α' martensite as a result of fast cooling rate exhibit a high tensile strength with a value of 1267 MPa [42]. This is because cooling rate is faster during selective laser melting solidification process (10^3–10^8 K/s) [53] than the critical cooling rate of Ti–6Al–4V martensitic transformation with the value of 410 K/s from β to α'. The near fully-dense SLM as-produced Ti–6Al–4V samples comprise microhardness of 409 Hv, which is higher than that of the samples manufactured by superplastic forming with a value of 346 Hv [54]. Furthermore, other mechanical properties, such as tensile UTS and yield properties, of the SLM-produced Ti–6Al–4V samples (Table 1) are higher than that of cast counterparts [26]. Corrosion resistance of SLM-produced sample is another important property. However, most the studies on selective laser melting process have mainly focused on the manufacturing process, densification and mechanical properties for as-produced parts. There is a lack of research into the corrosion behaviour of titanium parts (and other metallic materials) produced by selective laser melting. Recent studies have demonstrated the corrosion behaviour of SLM-produced Ti-6Al-4V in 3.5% NaCl solution compared to the commercial Grade 5 alloy [4, 52]. Potentiodynamic measurements pointed out that the corrosion

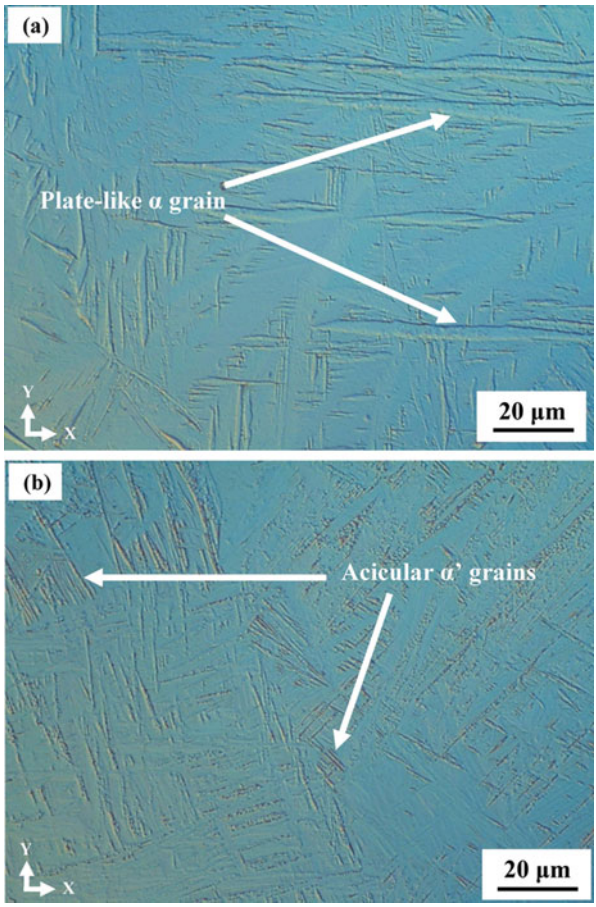

Fig. 5 Cross-sectional (Y-X) optical microstructure of the SLM-manufactured CP–Ti Samples, (**a**) Plate-like a and (**b**) acicular [9]

current density in the passive range of the SLM-produced Ti–6Al–4V alloy is twice that of the commercial Grade 5 alloy. This illustrates that the SLM-processed sample has worse corrosion resistance than the commercial Grade 5 alloy. The corrosion behavior of selective laser melted samples can also be affected by the building directions. Dai et al. revelled that XY-plane of SLM-produced sample had a greater corrosion resistance in comparison with XZ-plane in 1 M HCl solution, although having slight difference in 3.5 wt.% NaCl solution, pointing out that the different building planes presented more pronounced difference in corrosion resistance in harsher solution system [4]. Such a phenomenon was also found in SLM-produced Al-12Si alloy [61].

Recently, some β type titanium alloys produced by selective laser melting have been reported. Zhang et al. manufactured β type Ti2448 solid bulk parts by selective laser melting [16]. The relative density and micro-hardness generally increased with decreasing the laser scan speed, which corresponds to a higher laser energy density. Nearly full density samples (>99%) were obtained with a laser power of 200 W and a

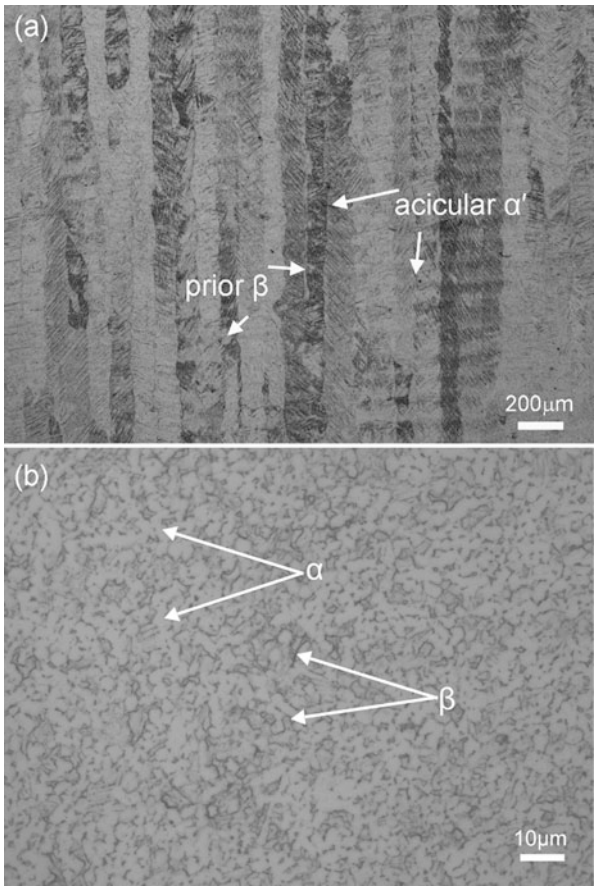

Fig. 6 Optical microstructure of the (**a**) SLM-produced Ti–6Al–4V sample and (**b**) Grade 5 alloy [52]

scan speed range of 300–600 mm/s. Compared with material prepared by conventional processing methods, SLM-produced samples with similar tensile property but without pronounced super-elastic properties as a result of the high oxygen content of the pre alloy powder. An example of a SLM-produced acetabular hip cup sample was completed with complex outer scaffold (Fig. 7). Liu et al. [10] reported an topology optimized porous structure with 85% porosity manufactured by Ti2448 material [10]. The relative density was influenced by laser scan speed and input energy. A high relative density specimen (>99%) was obtained under a scan speed of 750 mm/s and an input power of 175 W. The compressive strength reached ~51 MPa with a high ductility of ~14%. The results above showed that SLM-produced Ti2448 meets the requirement of implant in terms of mechanical properties. Very recently, the author also found that the topology optimized structure exhibits the excellent balance of bending and buckling stress with a high elastic energy absorption, a low Young's modulus (~2.3 GPa) and a high compressive strength (~58 MPa) [63].

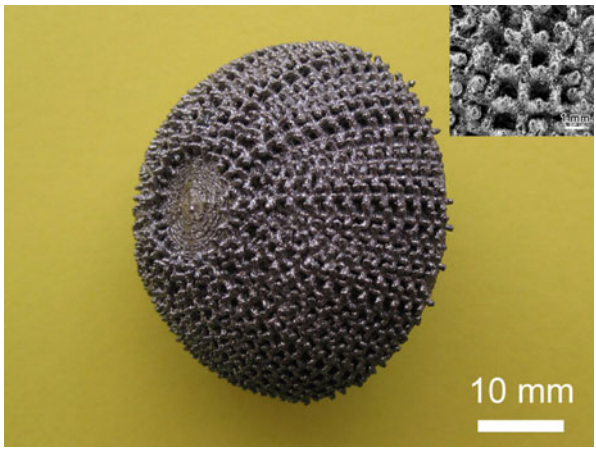

Fig. 7 An example of the SLM-produced precise Ti–24Nb–4Zr–8Sn acetabular cup [16]

3.2 Electron Beam Melting (EBM) of Titanium Alloys

Electron beam melting technology could process titanium components under a vacuum environment and obtain lower costs and more efficient production than conventional methods. Moreover, the advantages of electron beam melting include the ability to produce complex shapes to meet specific industry needs, as well as other advantages such as short processing cycles and efficient material utilization, making it an excellent alternative to titanium products. So far, Ti-6Al-4V alloy has been widely used as electron beam melting production. In order to improve the mechanical properties of the resulting components, extensive efforts have been made to optimize the process parameters to manipulate the microstructure of EBM-produced samples. Researches have also been conducted on another type of titanium alloy such as β-type Ti2448) [14, 30].

The microstructure of EBM as-produced Ti-6Al-4V is very complicated. In the electron beam melting process, the electron beam scans at high speed the powder bed and melts to generate a melt pool, and the liquid metal rapidly solidifies. As the building layers accumulate, the solidification of the solid part of the building below the building level is affected by the multiple thermal cycling effects in the vacuum environment due to lower cooling rates and heat build-up in the electron beam melting process. This results in the overall temperature of the sample being maintained at a high level, and this plays a key role in stress annealing elimination. Such a process facilitates good matching of sample strength and plasticity and uniformity of part performance [7, 14, 55–58]. The solid part of EBM as-produced Ti-6Al-4V contains columnar prior β grains which are delineated by α grain boundary and a transformed α/β structure, and Widmanstätten pattern and lamellar colony within the prior β grains [12, 41]. The generation of an α grain boundary along the grain boundaries of the prior β grains indicates the diffusive nature of the β-α transformation. In this way, the microstructure obtained in EBM-produced sample differs with the one observed in other AM-produced parts. Such as in selective laser

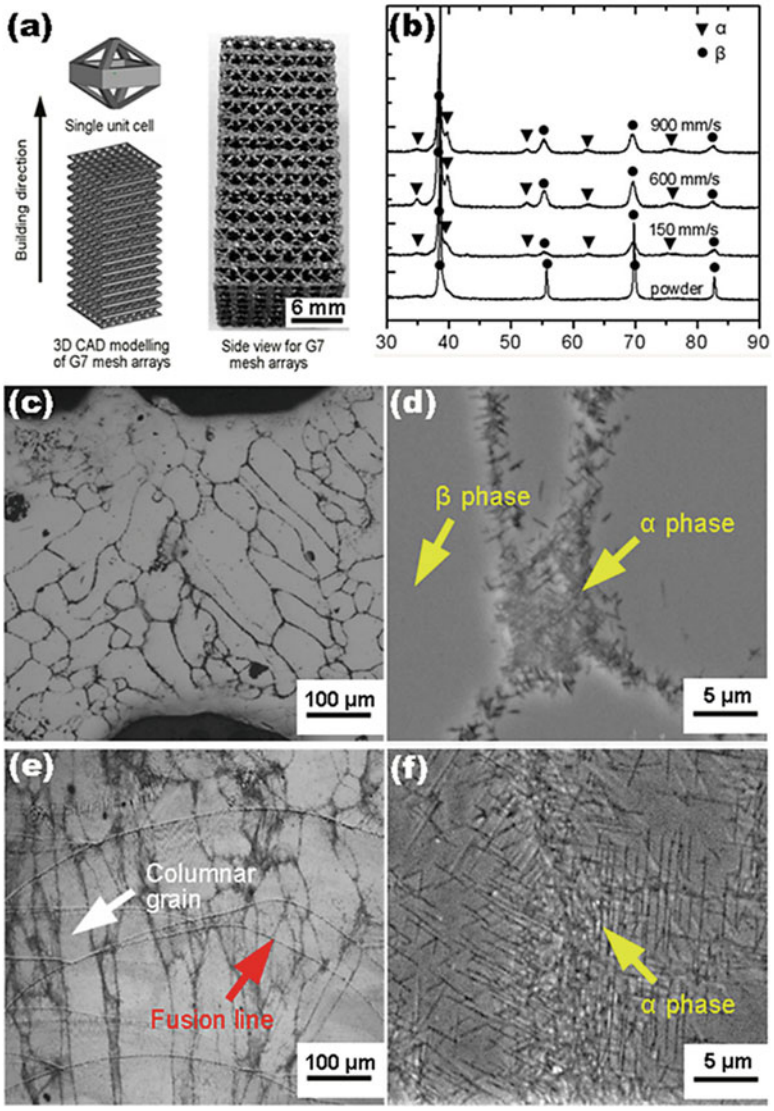

Fig. 8 (**a**) Porous structure model used and side view of EBM-processed Ti2448 component, (**b**) XRD profiles of the starting powder and EBM-processed components, (**c**) and (**e**) OM, and (**d**) and (**f**) SEM images of Group A. (**c**, **d**) are at horizontal plane and (**e**, **f**) are vertical views [6]

melting process with extremely fast cooling rates lead to a diffusion less martensitic β-α′ transformation. The texture of the parent β grain in EBM-produced sample exhibits a strong <001> β pole along the build direction (z axis) [5].

The EBM as-produced β titanium porous sample exhibits excellent properties. Fig. 8 shows the side view of EBM-processed, X-ray diffraction (XRD) patterns and

microstructure. Clearly, the EBM as-produced porous structure contained α phase due to a high temperature building environment and long time for cooling down. Liu et al. reported that the EBM-produced Ti2448 rhombic dodecahedron porous structures with a porosity of 70% exhibited great mechanical properties, for example, the ductility and the strength of the EBM as-produced sample are ~11% and ~37 MPa, respectively. The Young's modulus is only ~0.86 GPa, which is much lower than the Ti-6Al-4V rhombic dodecahedron porous samples with the same porosity (~1.4 GPa) [59]. EBM-processed Ti2448 porous samples have about two times of the strength-to-modulus ratio of the Ti-6Al-4V porous structures with the same structure and porosity of 70% [7]. The study for both SLM- and EBM-produced Ti2448 samples in terms of building parameters, defects pores, microstructures and mechanical properties has been conducted [7]. It was reported that selective laser melting sample with a finer laser beam spot created a deeper melt pool with more defect pores than that of EBM-produced sample. The formation of defect pore was significantly affected by the tin vaporization during the manufacturing process. The defects with a size smaller than 50 μm had limited effect on the compressive properties of the porous samples, but could decrease the fatigue properties of the sample under the higher stress levels [7]. More results on the processing and mechanical performance of the EBM-produced porous titanium structures have been summarized in our recent review article [30]. Very recently, it was reported that EBM-produced functionally graded Ti-6Al-4V alloy interconnected mesh structures show a combination of low density (0.5–2 g/cm3), high fatigue strength (~70 MPa) and energy absorption (~50 MJ/mg), which is superior to the ordinary uniform cellular structures [62].

4 Conclusion

This chapter summarizes the development of biomedical titanium for selective laser melting and electron beam melting. Biomedical titanium alloys such as Ti-6Al-4V are generally preferred materials for medical implants because of their low Young's modulus, superior biocompatibility, and high corrosion resistance compared to stainless steels and CoCr alloys. Porous structure can further improve the biocompatibility and reduce the Young's modulus of titanium alloy. Ti-24Nb-4Zr-8Sn (Ti2448) and other new biomedical titanium alloys with low modulus and non-toxic components will be the promisng material of choice for the next generation of biomedical implants.

Additive manufacturing (AM) technology based on titanium biomaterials has great potential in the medical industry. The complex structure made by AM provides enhanced mechanical properties and improved bone in-growth in the manufacture of artificial implants. Further research needs to focus on improving the roughness of AM implants by surface treatment, and reducing defects by optimizing building process. More studies are needed to prepare and fabricate for gradient porous structures with gradient Young's modulus to reduce the stress concentration of the

implants, and to design and manufacture more reliable implants that are more suitable for the human body and to bring better clinic results for patients.

References

1. Long M, Rack H (1998) Titanium alloys in total joint replacement—a materials science perspective. Biomaterials 19 (18):1621-1639
2. Gu DD, Meiners W, Wissenbach K, Poprawe R (2012) Laser additive manufacturing of metallic components: materials, processes and mechanisms. International Materials Review 57 (3):133-164.
3. Wang XJ, Xu SQ, Zhou SW, Xu W, Leary M, Choong P, Qian M, Brandt M, Xie YM (2016) Topological design and additive manufacturing of porous metals for bone scaffolds and orthopaedic implants: a review. Biomaterials 83:127-141
4. Dai N, Zhang LC, Zhang J, Zhang X, Ni Q, Chen Y, Wu M, Yang C (2016) Distinction in Corrosion Resistance of Selective Laser Melted Ti-6Al-4V Alloy on Different Planes. Corrosion Science 111:703-710
5. de Formanoir C, Michotte S, Rigo O, Germain L, Godet S (2016) Electron beam melted Ti–6Al–4V: Microstructure, texture and mechanical behavior of the as-built and heat-treated material. Materials Science and Engineering: A 652:105-119
6. Liu YJ, Li SJ, Hou WT, Wang SG, Hao YL, Yang R, Sercombe TB, Zhang LC (2016) Electron beam melted beta-type Ti-24Nb-4Zr-8Sn porous structures with high strength-to-modulus ratio. Journal of Materials Science & Technology 32 (6):505-508
7. Liu YJ, Li SJ, Wang HL, Hou WT, Hao YL, Yang R, Sercombe TB, Zhang LC (2016) Microstructure, defects and mechanical behavior of beta-type titanium porous structures manufactured by electron beam melting and selective laser melting. Acta Materialia 113:56-67
8. Attar H, Bönisch M, Calin M, Zhang LC, Scudino S, Eckert J (2014) Selective laser melting of in situ titanium–titanium boride composites: Processing, microstructure and mechanical properties. Acta Materialia 76 (9):13–22
9. Attar H, Calin M, Zhang LC, Scudino S, Eckert J (2014) Manufacture by selective laser melting and mechanical behavior of commercially pure titanium. Materials Science and Engineering: A 593:170-177
10. Liu YJ, Li X, Zhang LC, Sercombe T (2015) Processing and properties of topologically optimised biomedical Ti–24Nb–4Zr–8Sn scaffolds manufactured by selective laser melting. Materials Science and Engineering: A 642:268-278
11. Attar H, Löber L, Funk A, Calin M, Zhang LC, Prashanth KG, Scudino S, Zhang YS, Eckert J (2015) Mechanical behavior of porous commercially pure Ti and Ti-TiB composite materials manufactured by selective laser melting. Materials Science Engineering: A 625:350-356
12. Tan XP, Kok YH, Tan YJ, Descoins M, Mangelinck D, Tor SB, Leong KF, Chua CK (2015) Graded microstructure and mechanical properties of additive manufactured Ti–6Al–4V via electron beam melting. Acta Materialia 97:1-16
13. Zhao XL, Li SJ, Zhang M, Liu YD, Sercombe TB, Wang SG, Hao YL, Yang R, Murr LE (2016) Comparison of the microstructures and mechanical properties of Ti–6Al–4V fabricated by selective laser melting and electron beam melting. Materials & Design 95:21-31
14. Liu YJ, Wang HL, Li SJ, Wang SG, Wang WJ, Hou WT, Hao YL, Yang R, Zhang LC (2017) Compressive and fatigue behavior of beta-type titanium porous structures fabricated by electron beam melting. Acta Materialia 126:58-66
15. Chua CK, Leong KF (2015) 3D printing and additive manufacturing: principles and applications

16. Zhang LC, Klemm D, Eckert J, Hao YL, Sercombe TB (2011) Manufacture by selective laser melting and mechanical behavior of a biomedical Ti–24Nb–4Zr–8Sn alloy. Scripta Materialia 65 (1):21-24
17. Liu ZH, Zhang DQ, Chua CK, Leong KF (2013) Crystal structure analysis of M2 high speed steel parts produced by selective laser melting. Materials Characterization 84 (10):72–80
18. Ramirez DA, Murr LE, Martinez E, Hernandez DH, Martinez JL, Machado BI, Medina F, Frigola P, Wicker RB (2011) Novel precipitate-microstructural architecture developed in the fabrication of solid copper components by additive manufacturing using electron beam melting. Acta Materialia 59 (10):4088-4099
19. Sun SH, Koizumi Y, Kurosu S, Li YP, Chiba A (2015) Phase and grain size inhomogeneity and their influences on creep behavior of Co–Cr–Mo alloy additive manufactured by electron beam melting. Acta Materialia 86:305–318
20. Riedlbauer D, Drexler M, Drummer D, Steinmann P, Mergheim J (2014) Modelling, simulation and experimental validation of heat transfer in selective laser melting of the polymeric material PA12. Computational Materials Science 93:239-248
21. Wilkes J, Hagedorn Y-C, Meiners W, Wissenbach K (2013) Additive manufacturing of ZrO2-Al2O3 ceramic components by selective laser melting. Rapid Prototyping Journal 19 (1):51-57
22. Prashanth K, Scudino S, Klauss H, Surreddi KB, Löber L, Wang Z, Chaubey A, Kühn U, Eckert J (2014) Microstructure and mechanical properties of Al–12Si produced by selective laser melting: Effect of heat treatment. Materials Science and Engineering: A 590:153-160
23. Hrabe NW, Heinl P, Flinn B, Körner C, Bordia RK (2011) Compression-compression fatigue of selective electron beam melted cellular titanium (Ti-6Al-4V). Journal of Biomedical Materials Research Part B: Applied Biomaterials 99 (2):313-320
24. Lin CY, Wirtz T, LaMarca F, Hollister SJ (2007) Structural and mechanical evaluations of a topology optimized titanium interbody fusion cage fabricated by selective laser melting process. Journal of Biomedical Materials Research Part A 83 (2):272-279
25. Zhang LC, Attar H (2016) Selective laser melting of titanium alloys and titanium matrix composites for biomedical applications: a review. Advanced Engineering Materials 18 (4):463-475
26. Thijs L, Verhaeghe F, Craeghs T, Van Humbeeck J, Kruth JP (2010) A study of the microstructural evolution during selective laser melting of Ti–6Al–4V. Acta Materialia 58 (9):3303-3312
27. Parthasarathy J, Starly B, Raman S, Christensen A (2010) Mechanical evaluation of porous titanium (Ti6Al4V) structures with electron beam melting (EBM). Journal of the Mechanical Behavior of Biomedical Materials 3 (3):249-259
28. Mohammadhosseini A, Masood SH, Fraser D, Jahedi M (2015) Dynamic compressive behaviour of Ti-6Al-4V alloy processed by electron beam melting under high strain rate loading. Advanced Manufacturing 3 (3):232-243
29. Murr LE, Gaytan SM, Ceylan A, Martinez E, Martinez JL, Hernandez DH, Machado BI, Ramirez DA, Medina F, Collins S (2010) Characterization of titanium aluminide alloy components fabricated by additive manufacturing using electron beam melting. Acta Materialia 58 (5):1887-1894
30. Zhang LC, Liu YJ, Li SJ, Hao YL (2018) Additive manufacturing of titanium alloys by electron beam melting: a review. Advanced Engineering Materials 20 (5):1700842
31. Zhang H, Lewis CG, Aronow MS, Gronowicz GA (2004) The effects of patient age on human osteoblasts' response to Ti–6Al–4V implants in vitro. Journal of Orthopaedic Research 22 (1):30-38
32. Johansson CB, Albrektsson T, Ericson LE, Thomsen P (1992) A quantitative comparison of the cell response to commercially pure titanium and Ti-6Al-4V implants in the abdominal wall of rats. Journal of Materials Science Materials in Medicine 3 (2):126-136
33. Haghighi SE, Lu H, Jian G, Cao G, Habibi D, Zhang LC (2015) Effect of α ″martensite on the microstructure and mechanical properties of beta-type Ti–Fe–Ta alloys. Materials & Design 76:47-54

34. Rao S, Okazaki Y, Tateishi T, Ushida T, Ito Y (1997) Cytocompatibility of new Ti alloy without Al and V by evaluating the relative growth ratios of fibroblasts L929 and osteoblasts MC3T3-E1 cells. Materials Science and Engineering: C 4 (4):311-314
35. Niinomi M, Nakai M, Hieda J (2012) Development of new metallic alloys for biomedical applications. Acta Biomaterialia 8 (11):3888-3903
36. Eisenbarth E, Velten D, Müller M, Thull R, Breme J (2004) Biocompatibility of β-stabilizing elements of titanium alloys. Biomaterials 25 (26):5705-5713
37. Zardiackas LD, Mitchell DW, Disegi JA (1996) Characterization of ti-15Mo Beta Titanium Alloy for Orthopaedic. Medical Applications of Titanium and Its Alloys: The Material and Biological Issues (1272):60
38. Ho W, Ju C, Lin JC (1999) Structure and properties of cast binary Ti–Mo alloys. Biomaterials 20 (22):2115-2122
39. Kim H, Ikehara Y, Kim J, Hosoda H, Miyazaki S (2006) Martensitic transformation, shape memory effect and superelasticity of Ti–Nb binary alloys. Acta Materialia 54 (9):2419-2429
40. Hao Y, Li S, Sun S, Yang R (2006) Effect of Zr and Sn on Young's modulus and superelasticity of Ti–Nb-based alloys. Materials Science and Engineering: A 441 (1):112-118
41. Al-Bermani SS, Blackmore ML, Zhang W, Todd I (2010) The origin of microstructural diversity, texture, and mechanical properties in electron beam melted Ti-6Al-4V. Metallurgical and Materials Transaction A 41 (13):3422-3434
42. Vrancken B, Thijs L, Kruth J-P, Van Humbeeck J (2012) Heat treatment of Ti6Al4V produced by Selective Laser Melting: Microstructure and mechanical properties. Journal of Alloys and Compounds 541:177-185
43. Facchini L, Magalini E, Robotti P, Molinari A (2009) Microstructure and mechanical properties of Ti-6Al-4V produced by electron beam melting of pre-alloyed powders. Rapid Prototyping Journal 15 (3):171-178
44. Gaytan SM, Murr LE, Medina F, Martinez E, Lopez MI, Wicker RB (2009) Advanced metal powder based manufacturing of complex components by electron beam melting. Materials Technololgy 24:180-190
45. Murr LE, Esquivel EV, Quinones SA, Gaytan SM, Lopez MI, Martinez EY, Medina F, Hernandez DH, Martinez E, Martinez JL (2009) Microstructures and mechanical properties of electron beam-rapid manufactured Ti-6Al-4V biomedical prototypes compared to wrought Ti–6Al–4V. Materials Characterization 60 (2):96-105
46. Koike M, Martinez K, Guo L, Chahine G, Kovacevic R, Okabe T (2011) Evaluation of titanium alloy fabricated using electron beam melting system for dental applications. Journal of Materials Processing Technology 211 (8):1400-1408
47. Scharowsky T, Juechter V, Singer RF, Körner C (2015) Influence of the scanning strategy on the microstructure and mechanical properties in selective electron beam melting of Ti–6Al–4V. Advanced Engineering Materials 17 (11):1573-1578
48. Baudana G, Biamino S, Klöden B, Kirchner A, Weißgärber T, Kieback B, Pavese M, Ugues D, Fino P, Badini C (2016) Electron beam melting of Ti-48Al-2Nb-0.7 Cr-0.3 Si: feasibility investigation. Intermetallics 73:43-49
49. Hernandez J, Li SJ, Martinez E, Murr LE, Pan XM, Amato KN, Cheng XY, Yang F, Terrazas CA, Gaytan SM (2013) Microstructures and Hardness Properties for β-Phase Ti-24Nb-4Zr-7.9 Sn Alloy Fabricated by Electron Beam Melting. Journal of Materials Science & Technology 29 (11):1011-1017
50. Imanishi J, Choong PF (2015) Three-dimensional printed calcaneal prosthesis following total calcanectomy. International Journal of Surgery Case Reports 10:83-87
51. Gu D, Hagedorn Y-C, Meiners W, Meng G, Batista RJS, Wissenbach K, Poprawe R (2012) Densification behavior, microstructure evolution, and wear performance of selective laser melting processed commercially pure titanium. Acta Materialia 60 (9):3849-3860
52. Dai N, Zhang LC, Zhang J, Chen Q, Wu M (2016) Corrosion Behaviour of Selective Laser Melted Ti-6Al-4V Alloy in NaCl Solution. Corrosion Science 102:484-489

53. Das M, Balla VK, Basu D, Bose S, Bandyopadhyay A (2010) Laser processing of SiC-particle-reinforced coating on titanium. Scripta Materialia 63 (4):438-441
54. Niinomi M (1998) Mechanical properties of biomedical titanium alloys. Materials Science and Engineering: A 243 (1):231-236
55. Suo J, Chen H, Li Z (2009) Mechanical Properties of Ti-6Al-4V Alloys by Electron Beam Melting (EBM)[J]. Aerospace Manufacturing Techology 6:6
56. Malinauskas M, Rekštytė S, Lukoševičius L, Butkus S, Balčiūnas E, Pečiukaitytė M, Baltriukienė D, Bukelskienė V, Butkevičius A, Kucevičius P (2014) 3D Microporous Scaffolds Manufactured via Combination of Fused Filament Fabrication and Direct Laser Writing Ablation. Micromachines 5 (4):839-858
57. Bai Y, Gai X, Li SJ, Zhang LC, Liu YJ, Hao YL, Zhang X, Yang R, Gao YB (2017) Improved corrosion behaviour of electron beam melted Ti-6Al–4 V alloy in phosphate buffered saline. Corrosion Science 123:289-296
58. Zhao S, Li SJ, Hou WT, Hao YL, Yang R, Misra RDK (2016) The influence of cell morphology on the compressive fatigue behavior of Ti-6Al-4V meshes fabricated by electron beam melting. Journal of the Mechanical Behavior of Biomedical Materials 59:251-264
59. Kufelt O, Eltamer A, Sehring C, Schliewolter S, Chichkov BN (2014) Hyaluronic acid based materials for scaffolding via two-photon polymerization. Biomacromol 15 (2):650-659
60. Liu YJ, Liu Z, Jiang Y, Wang GW, Yang Y, Zhang LC (2018) Gradient in microstructure and mechanical property of selective laser melted AlSi10Mg. Journal of Alloys and Compounds 735:1414-1421
61. Chen Y, Zhang J, Gu X, Dai N, Qin P, Zhang LC (2018) Distinction of corrosion resistance of selective laser melted Al-12Si alloy on different planes. Journal of Alloys and Compounds 747:648-658
62. Zhao S, Li SJ, Wang SG, Hou WT, Li Y, Zhang LC, Hao YL, Yang R, Misra RDK, Murr LE (2018) Compressive and fatigue behavior of functionally graded Ti-6Al-4V meshes fabricated by electron beam melting. Acta Materialia 150:1-15
63. Liu YJ, Li SJ, Zhang LC, Hao YL, Sercombe TB (2018) Early plastic deformation behaviour and energy absorption in porous β-type biomedical titanium produced by selective laser melting. Scripta Materialia 153:99-103